Activation of Phosphodiesterase by Transducin in Bovine Rod Outer Segments: Characteristics of the Successive Binding of Two Transducins

Franz Bruckert,[‡] Patrice Catty,[§] Philippe Deterre,[∥] and Claude Pfister*

Laboratoire de Biophysique Moléculaire et Cellulaire, Département de Biologie Moléculaire et Structurale, Centre d'Etudes Nucléaires, BP 85 X/38041 Grenoble Cedex, France

Received March 29, 1994; Revised Manuscript Received July 18, 1994[⊗]

ABSTRACT: In bovine retinal rods, transducin loaded with GTP or GTPγS (T*) activates a cGMP phosphodiesterase (PDE) by forming a tightly membrane-bound complex with it [Catty, P., et al. (1992) *J. Biol. Chem. 267*, 19489–19493]. Up to two T*s are able to bind to PDE [Clerc, A., & Bennett, N. (1992) *J. Biol. Chem. 267*, 6620–6627]. We analyze here PDE activation by two successive bindings of T*. In the mathematical model used, we took into account that the membrane concentration determines the amount of PDE able to interact efficiently with T* through the attachment of PDE itself to the membrane. We therefore fitted the data obtained over a wide range of membrane and PDE concentrations. We found that the binding of the first T* to PDE elicits 80–100% of the maximal activity of PDE, whereas the binding of the second T* to PDE elicits little or no additional activation of PDE. This finding profoundly differs from previous conclusions. The carefully controlled conditions of our experiments permit one to understand these discrepancies. In the physiological situation, PDE would be nearly maximally activated through its interaction with only one T*. The efficient binding of the second T* to those complexes would then ensure a rapid deactivation of T* through the enhancement of the rate of GTP hydrolysis in T* bound to PDE [Pagès, F., et al. (1992) *J. Biol. Chem. 267*, 22018–22021; Pagès, F., et al. (1993) *J. Biol. Chem. 268*, 26358–26364].

Vertebrate photoreceptors respond to incident light through a cascade of events occurring in the outer segment. Light is initially captured at the level of rhodopsin (Rh),[1] and the plasma membrane of the photoreceptor is ultimately hyperpolarized by the closure of cationic channels. This is achieved via the decrease of the concentration of intracellular cyclic GMP, catalyzed by a cGMP phosphodiesterase (PDE). The link between photoexcited rhodopsin and phosphodiesterase involves an heterotrimeric GTP-binding protein, transducin (T): T interacts with photoexcited rhodopsin and exchanges bound GDP for GTP on its α-subunit (Tα). This Tα subunit loaded with GTP, hereinafter named T*, is the direct activator of PDE [reviewed, for instance, by Chabre and Deterre (1989), Stryer (1991), and Pfister et al. (1993)].

PDE consists of a catalytic core, PDEαβ (PDEα, 100 kDa; PDEβ, 98 kDa; one copy of each per molecule of PDE), and inhibitory subunits (PDEγ, 9.7 kDa; two copies per molecule of PDE). Numerous studies have described some characteristics of the activation of PDE by T* [reviewed in Pfister et al. (1993)]. T* activates PDE by relieving the inhibitory constraints imposed on PDEαβ by PDEγ. This implies direct interactions between T* and PDEγ. In the presence of membranes, two T*s are able to bind to one PDE during maximal activation (Clerc & Bennett, 1992). The complex thus formed appears to bind to the membranes more tightly than PDE alone (Catty et al., 1992). In the absence of membranes, the activation of PDE has been ascribed to a physical removal of PDEγ by T*, to form PDEαβ (active species) and T*–PDEγ complexes (Wensel & Stryer, 1986; Deterre et al., 1986). The presence or absence of membranes would then lead to two different molecular mechanisms of PDE activation, and this could explain the differences in efficiency of T* in the two corresponding conditions: in the presence of membranes, submicromolar amounts of T* are able to activate PDE, whereas in their absence at least 10 μM T* is required (Fung & Nash, 1983; Tyminski & O'Brien, 1984; Liebman & Sitaramayya, 1984; Bennett & Clerc, 1989).

Bennett and Clerc (1989) and Clerc et al. (1992) report quantitative analyses of the activation of PDE by the successive binding of two T*s in the presence of membranes. It was deduced that the two apparent binding constants of T* to PDE would be about 0.1 and 0.6 μM, respectively (Bennett & Clerc, 1989), or 0.075 and 0.22 μM (Clerc et al., 1992). Most interestingly, the binding of the first T* would elicit only a very low specific activity in PDE (30% of the maximal activity). The binding of the second T* to PDE was then thought to be necessary to elicit full activity of PDE. Although membranes were indeed present in these assays, the influence of their concentration on the membrane binding of PDE and the formation of its complexes with T* were not considered. In some of the experiments, one suspects that only part of PDE was membrane-bound and therefore readily activatable at the concentration of T* added.

The quantitative analysis reported here on the activation of PDE by T* includes the concentration of membranes as a parameter of the activation reaction. In this study, we used a wide range of membrane, PDE, and T* concentrations. Under

* To whom correspondence should be addressed at Institut de Biologie Structurale, 41 Avenue des Martyrs, 38027 Grenoble Cedex 01, France. Telephone: (33) 76 88 95 70. Fax: (33) 76 88 54 94.

‡ Present address: Program in Cellular Biochemistry and Biophysics, Rockefeller Research Laboratories, Sloan-Kettering Institute, 1275 York Ave., Box 251, New York, New York 10021.

§ Present address: Université Catholique de Louvain, Biochimie Physiologique, Place Croix du Sud 2-20, 1348 Louvain la Neuve, Belgium.

∥ Present address: Immunologie Cellulaire et Tissulaire, Bâtiment CERVI, Hôpital de la Pitié-Salpétrière, 83, Bvd de l'Hôpital, 75651 Paris Cedex 13, France.

⊗ Abstract published in *Advance ACS Abstracts,* September 15, 1994.

[1] Abbreviations: ROS, rod outer segments; Rh, rhodopsin; Rh*, photoexcited Rh; T, transducin; Tα, Tβ, Tγ, subunits of T; T*, Tα loaded with GTP or GTPγS; GTPγS, guanosine 5′-*O*-(thiotriphosphate); PDE, 3′,5′-cyclic GMP-specific phosphodiesterase; PDEα, PDEβ, PDEγ, subunits of PDE.

0006-2960/94/0433-12625$04.50/0

most conditions, activation of PDE occurred only on membranes, when PDE was involved in membrane-bound complexes with T*. Our data suggest that, under these conditions, the binding of the first T* induces a nearly maximal activation of PDE (80–100% of maximum). The second T* then binds more efficiently to T*–PDE than the first T* to PDE, but brings little or no additional activation to PDE.

EXPERIMENTAL PROCEDURES

Buffers. Isotonic buffer was 20 mM Hepes, 120 mM NaCl, and 2 mM $MgCl_2$, pH 7.5. Hypotonic buffer was 5 mM Hepes, pH 7.5. Prior to use, all buffers were degassed by argon bubbling and complemented with 0.1 mM phenylmethanesulfonyl fluoride and 2 mM β-mercaptoethanol.

Preparation of ROS and Washed Membranes. ROS were prepared under ambient light from bovine eyes collected shortly after sacrifice and were purified by sucrose flotation (Kühn, 1981).

Hereinafter, "native membranes" will refer to suspensions of ROS containing their intrinsic pool of PDE (and of inactive transducin, which is not involved in the experiments, unless stated otherwise). "Washed membranes" were obtained by extensive washing of ROS suspensions (12.5 μM Rh), once in hypotonic buffer, then in hypotonic buffer supplemented with GTP to completely remove transducin, and finally three times in isotonic buffer. These washed membranes therefore essentially contain rhodopsin and are devoid of T and PDE.

The concentration of membranes in the suspensions is inferred from the corresponding concentration of rhodopsin. This was determined spectroscopically from the absorbance of the suspension in the presence of a detergent (ammonyx) and of hydroxylamine. Because the suspension contains photoexcited rhodopsin, retinal oxyme is formed and absorbs at 365 nm. The molar extinction coefficient was taken as 47×10^3 M^{-1} cm^{-1}.

*Extraction and Purification of PDE and T**. The procedure was as in Catty et al. (1992). Briefly, bleached membranes were suspended in isotonic buffer (12.5 μM Rh) and centrifuged. The supernatant (soluble proteins) was then discarded, and the pellet was resuspended in hypotonic buffer. Centrifugation yielded a supernatant designated "crude PDE". The pellet was then resuspended in isotonic buffer supplemented with GTPγS, and centrifugation yielded a "crude T*" supernatant. These extraction procedures were also used to determine the PDE and transducin content of a ROS suspension.

Purification of the proteins was carried out by anion-exchange chromatography (FPLC-Pharmacia polyanion SI column, eluted with a Na_2SO_4 gradient, as described by Deterre et al. (1984, 1986) and used in Catty et al. (1992). The proteins were then desalted by gel filtration on PD-10 columns (Pharmacia), concentrated using Diaflo and/or Centricon systems (Amicon), and used within 1 day. Before use, they were stored at 4 °C in the presence of 0.1 mM NaN_3. Freeze-thawing procedures were avoided to limit protein degradation.

Determination of T and PDE Concentrations in Solution (Crude or Purified Extracts).* The total protein concentration was measured by the colorimetric Coomassie Blue assay (Bradford Dye reagent from Bio-Rad) using BSA as a standard. When necessary, the solution was electrophoresed (Laemmli gel, 12.5% acrylamide), and the percentage of the protein of interest was determined from scans of Coomassie Blue stained gels. Correction factors for staining differences of T* or PDE relative to BSA (Compton & Jones, 1985) were derived from the amino acid sequences of the proteins and were respectively 0.7 and 0.8. As these values were very similar, they did not influence the calculation of the apparent binding constants from the experimental data, and this correction was omitted.

Determination of the Partitioning of PDE between Membranes and Solution. A sample consisting of a suspension in isotonic buffer of membranes, PDE, and, when appropriate, T* at the desired concentrations was incubated for 5 min at 24 °C to allow the proteins to partition between membranes and solution and was then centrifuged (36000*g*, 5 min). The supernatant (S_1) contained the "soluble" fraction of PDE, and the pellet (P_1) contained "membrane-bound" PDE. The determination of soluble PDE in S_1 was carried out either by protein determination (Bradfords and gel scans; see above) or by measuring the PDE activity obtained after trypsin treatment of the solution (see below). The amount of membrane-bound PDE was determined in either of the following ways. For the first method, the P_1 pellet was suspended in hypotonic buffer, and PDE was extracted by centrifugation. The procedure was repeated twice, yielding supernatants S_2 and S_3 and leaving less than 10% of the initial PDE in the suspension unextracted. PDE in the S_2 and S_3 supernatants was then measured as for S_1. As a second method, the P_1 pellet was resuspended in isotonic buffer and treated with trypsin (see below), and the PDE activity was measured. The two determinations gave identical data.

Trypsin Treatment of PDE-Containing Samples. For tryptic digestion in the absence of membranes (supernatants), trypsin (Worthington) was added to a final concentration of 10 μg/mL and the mixture was incubated for 25 min at 25 °C. The reaction was then stopped by addition of 400 μg/mL trypsin inhibitor (lima bean, Worthington) and 1 mM phenylmethanesulfonyl fluoride.

For digestion in the presence of membranes, trypsin was added to a final concentration of 15–45 μg/mL, and the reaction was allowed to proceed for 30 min at 25 °C before being stopped.

In both cases, the PDE activity obtained [2000–2300 cGMP/(s PDE)] was constant in the chosen range of incubation conditions (Catty & Deterre, 1991) and similar to the specific activity reported in Bennett and Clerc (1989).

PDE Assays. PDE assays were carried out in isotonic buffer. cGMP hydrolysis was monitored by the change of the suspension pH (Liebman & Evanczuk, 1981) in a microcuvette thermostated at 25 °C. The ROS suspension, or the reconstituted system of washed membranes and PDE, was supplemented with T*, yielding a total volume of 380 μL at an initial pH of 7.5 ± 0.1. Under continuous stirring, 20 μL of a cGMP solution (final concentration, 4–8 mM) was injected at time 0. The mixing of cGMP was complete within 3 s, as determined from a control experiment in which 20 μL of HCl was mixed with the assay buffer. This transient time of mixing was the same at all membrane concentrations used here and was not considered in the analysis. The slope of the pH change was thereafter constant, and its value could be determined, provided this linear phase extended for at least 3 s. This allowed us to measure hydrolytic activities as high as 1 mM cGMP/s. The total amplitude of the pH variation due to cGMP hydrolysis never exceeded 0.2 pH units, and it was independent of the concentration of membranes or proteins in the assay. The specific activity data (moles of cGMP hydrolyzed by 1 mole of PDE in 1 s) are given the unit cGMP/(s PDE).

All of the experimental data originate from 2–5 independent experiments. The reproducibility of the results was better than 10%. In the mathematical modeling of the activation curves, it appeared more meaningful to analyze a complete set of experiments, obtained from a single stock of membrane and T*, than to analyze a mean of independent experiments with their detectable although minor quantitative variabilities. One set of experiments, with the four membrane concentrations tested (from 2.5 to 150 μM Rh), was therefore performed from a single stock preparation of membranes and of T*.

MATHEMATICAL MODELS

Three characteristics of the activation of PDE by T* are fundamental for our modeling. First, two T*'s can interact with PDE. Second, the efficiency of T* in activating PDE is dependent upon the presence of membranes. Third, in an actual experiment, both the attachment of PDE itself to the membrane and the interaction of PDE with T* contribute to the observed activity of PDE as well as to its overall membrane binding. The model must therefore account for all of these characteristics, which will be detailed separately. Moreover, we will assume that all T*s added are in a monomeric and fully active form (see Discussion).

*Binding of PDE to the Membranes in the Absence of T**. The association of PDE with the membranes is modeled here by the binding of PDE to nonspecific "sites" on the membrane (total concentration of sites, B_{tot}). The equilibrium constant, K_{PDE}, is then

$$K_{PDE} = \frac{[PDE_{sol}](B_{tot} - [PDE_{mb}])}{[PDE_{mb}]} \quad (1)$$

where PDE_{sol} and PDE_{mb} are the soluble and membrane-bound fractions of PDE, respectively.

Binding of T to PDE*. Two "loci" for binding of T* are supposed to exist on PDE. These loci involve the two PDEγs present in the PDE holoenzyme PDE$\alpha\beta\gamma_2$ (Deterre et al., 1988; Fung et al., 1990; Clerc & Bennett, 1992). The structural model for PDE is often represented for simplicity as though one PDEγ interacted with PDEα, and the other, with PDEβ [reviewed in Pfister et al. (1993)]. Indeed, PDEα and PDEβ subunits are very similar [72% homology; see Lipkin et al. (1990)], and the two PDEγs are described as having identical binding characteristics (Wensel & Stryer, 1990; Deterre et al., 1988). We therefore postulate here that the two loci for the binding of the first T* on PDE also share identical characteristics: the formation of the complexes T*–PDE$\alpha\gamma$–PDE$\beta\gamma$ and PDE$\alpha\gamma$–PDE$\beta\gamma$–T* may therefore be described by a single apparent binding constant. These complexes will be referred to as T*–PDE. The binding of the second T* to T*–PDE then yields a complex which will be named T*–PDE–T*, and this binding will also be characterized by a single apparent constant, irrespective of the domain of PDE concerned. In the absence of detailed structural data, this appears to be the simplest model, as already used by Bennett and Clerc (1989) and Clerc et al. (1992).

In our experimental conditions, no PDE activity was recovered in solution (see below); therefore we assumed that only membrane-bound PDE was involved in complexes with T*, and we considered the following two successive equilibria:

$$PDE_{mb} + 2T^*_{free} \overset{K_1}{\leftrightarrow} T^*\text{–}PDE_{mb} + T^*_{free} \overset{K_2}{\leftrightarrow} T^*\text{–}PDE_{mb}\text{–}T^*$$

where K_1 and K_2 are the apparent affinities for each of these equilibria. PDE_{mb} represents the pool of free PDE that is bound to the membrane, and T^*_{free}, the pool of T* not complexed to PDE.

PDE Activation and the Effect of Membranes. In most of the experiments described in this work, i.e., for membrane concentrations at or above 2.5 μM Rh, our results are apparantly consistent with the assumption that, as far as PDE activation is concerned, only the subpool of PDE which is membrane-bound has to be taken into consideration. It is well known that activation of PDE in solution requires much higher T* concentrations than in the presence of membranes [see, for instance, Bennett & Clerc (1989)]. Therefore, in the membrane concentration range when most of the PDE is membrane-bound in the absence of T* (i.e., above about 25 μM Rh), the absence of a noticeable PDE activity in solution is clear. At lower membrane concentrations (about 2.5–25 μM Rh), PDE is only partially membrane-bound in the absence of T*, but addition of T* leads to a decrease of the pool of soluble PDE through the formation of membrane-bound complexes (Catty et al., 1992). As a result, little or no activated PDE appears in the small percentage of PDE remaining in the soluble fraction. Indeed, we never recovered more than 1–5% of PDE activity in the supernatant after centrifugation of a ROS suspension supplemented with T*.

The experimental activity data (A) are related to the specific activities a_1 and a_2 of the T*–PDE_{mb} and T*–PDE_{mb}–T* complexes, respectively, as

$$A = a_1[T^*\text{–}PDE_{mb}] + a_2[T^*\text{–}PDE_{mb}\text{–}T^*]$$

At high concentrations of T* (10–15 μM T*; see Results), when all of the PDEs are complexed to T* in the T*–PDE–T* form, the activity reaches its maximum a_2 [PDE_{tot}]. The partial activation of PDE in the T*–PDE complex, a_1/a_2, is a number between 0 and 1, referred to hereinafter as α.

*Modeling of PDE Activation in a ROS Suspension Supplemented with T**. In this section, we relate the PDE activity A, measured in the presence of membranes, of PDE (PDE_{tot}) and of T* (T_{tot}), to the amount of free membrane-bound PDE (PDE_{mb}) and to the amount of free T* (T^*_{free}) existing under the given experimental conditions.

PDE (PDE_{tot}) exists as four different species: free soluble PDE (PDE_{sol}), free membrane-bound PDE (PDE_{mb}), and PDE complexed on the membrane to one T* (T*–PDE_{mb}) or to two T*s (T*–PDE_{mb}–T*). Using eq 1 and the apparent binding constants defined above,

$$[PDE_{tot}] = [PDE_{mb}]\left(1 + \frac{K_{PDE}}{B_{tot} - [PDE_{mb}]} + \frac{[T^*_{free}]}{K_1} + \frac{[T^*_{free}]^2}{K_1K_2}\right) \quad (2)$$

Transducin (T^*_{tot}) exists essentially in three forms: free (and soluble) transducin (T^*_{free}) and transducin in T*–PDE or T*–PDE–T* complexes. Therefore,

$$[T^*_{tot}] = [T^*_{free}] + [PDE_{mb}]\left(\frac{[T^*_{free}]}{K_1} + 2\frac{[T^*_{free}]^2}{K_1K_2}\right) \quad (3)$$

We observed that some T^*_{free} could be "trapped" by the membranes and was unable to take part in the PDE activation process. The corresponding term [$T^*_{trapped}$] was typically 25 nM at a ROS concentration of 50 μM Rh (see Figure 4B in the Results, section C), and a corresponding correction was applied to [T^*_{tot}] in the low concentration range.

The observed PDE activity (A) is then

$$A = [PDE_{mb}]\left(a_1\frac{[T^*_{free}]}{K_1} + a_2\frac{[T^*_{free}]^2}{K_1K_2}\right) \quad (4)$$

Mathematical Treatment of the Theoretical Activation Data. PDE activity, A, is expressed in eq 4 as a function of $[PDE_{mb}]$ and $[T^*_{free}]$. Via eqs 2 and 3, A is therefore an implicit function of the experimental parameters $[T^*_{tot}]$ and $[PDE_{tot}]$. Two programs were written in Mathematica software and run on a Macintosh II SI.

In a first program, A was expressed as a function of $[T^*_{tot}]$ at constant $[PDE_{tot}]$. This was relevant to fit the experiments in which various amounts of T^*_{tot} were added to ROS suspensions of constant membrane concentration and PDE content. The activity A obtained at a given concentration of T^*_{tot} was then normalized to that obtained under addition of excess T^*_{tot} to give $A_n = A/a_2[PDE_{tot}]$. The calculated values, A_n^{calc}, were then compared to A_n, and a mean-squares error E was calculated as

$$E^2 = \frac{\sum_{\text{all data points}} |A_n^{calc} - A_n|^2}{\text{number of data points}}$$

E^2 will be taken as a score for the fit: values under 50 are considered acceptable, as they correspond to deviations of less than about 10% at each experimental point.

In a second program, A was expressed as a function of $[PDE_{tot}]$ (or of a parameter related to it; see below) at constant $[T^*_{tot}]$. This was relevant to fit the experiments in which ROS at the same membrane concentration, but with different PDE contents, were supplemented with the same $[T^*_{tot}]$. It was used here in the case of low concentrations of T^*_{tot}, i.e., to describe the slope at the origin of the activation curve of PDE by T^*_{tot}. The activity A obtained at a given concentration of PDE_{tot} was here normalized to the maximum theoretical activity obtained with $[T^*_{tot}]$ as $A_n' = A/\{a_2([T^*_{tot}] - [T^*_{trapped}])\}$, where $T^*_{trapped}$ has been defined above. In the present case of low concentrations of T^*_{tot}, the calculated activity was almost insensitive to K_2, and we therefore used an approximate expression for A_n' containing only K_1 and α. The approximation of eqs 2 and 3 for $[T^*_{tot}] \rightarrow 0$, implying the value for $[T^*_{tot}] = 0$ of the first derivative of A with respect to $[PDE_{tot}]$, yields A as a function of $[PDE_{mb}^0]$ (the amount of PDE bound to nonspecific sites on the membranes in the absence of T*). A simple expression can thus be derived:

$$A_n' = \frac{\alpha[PDE_{mb}^0]}{K_1 + [PDE_{mb}^0]} \quad (5)$$

We tested the validity of this approximation by comparing the theoretical activation curves obtained through eq 5 and through the complete set of eqs 2–4. We found that this expression is valid as long as K_2 is not much lower than K_1 (typically if $K_2 > 0.1K_1$) and if $[T^*_{tot}]$ is lower than K_2 (typically, $[T^*_{tot}] < K_2$).

RESULTS

The determination of the apparent affinities of T* for PDE and the corresponding activation characteristics of PDE are strongly dependent upon the exact knowledge of the concentration of the molecular species. This requires that one not only determine the protein concentration by colorimetric methods but also check which portion of these proteins is "potent" for the activation under study. Therefore, the first part of this study deals with the limits of validity of our reconstitution procedures. Moreover, when PDE activation has been tested in the presence of membranes, evidence has shown that the soluble and membrane-bound pools of PDE contribute differently to the observed activity induced by T* in the ROS suspension (Fung & Nash, 1983; Tyminski & O'Brien, 1984; Liebman & Sitaramayya, 1984; Bennett & Clerc, 1989). Therefore, the second part of this report gives data allowing quantification of the amount of PDE bound to the membranes. Finally, in a third part, our experiments will be analyzed with respect to the activation of PDE by T*.

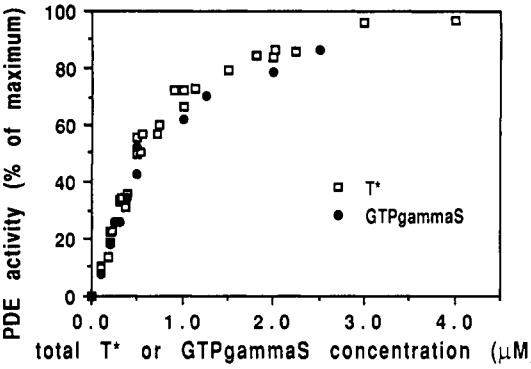

FIGURE 1: Activation of endogenous PDE by purified or endogenous T*. Native ROS suspensions (final concentration, 50 μM Rh) were complemented with either purified T* (the Tα subunit of transducin loaded with GTPγS (□) or with GTPγS (●). Final concentrations are indicated on the abscissa. The data are from two independent experiments.

(A) Limits of Validity of Reconstitution Experiments. (i) "Potency" of Extracted/Purified T To Activate PDE.* To address this question, we compared two experiments carried out on native ROS suspensions containing their endogenous PDE (Figure 1): (i) Activation of PDE obtained by addition of known amounts of exogenous extracted/purified T* (open squares). In this case, the endogenous transducins are not concerned. (ii) Activity of PDE obtained through activation of endogenous T by GTPγS (closed circles). In this case, after incubation with GTPγS, transducins of the endogenous pool of the ROS suspension are irreversibly activated by GTPγS present at a 1:1 stoichiometry. The concentration of T* is therefore equal to the concentration of added GTPγS, provided the latter does not exceed the concentration of available transducins (typically 2–3 μM at a ROS concentration of 50 μM Rh). Figure 1 shows that, in the range of T* concentrations tested, the PDE activities obtained in these two experiments are almost identical. In our experiments, purified T* appears therefore as potent as endogenous nonextracted T* for the activation of PDE. Under these conditions, we expect little or no heterogeneity in the T* preparation that could perturb our interpretation of the experimental data (see Discussion).

(ii) Potency of Extracted/Purified PDE To Be Activated by T.* Exogenous PDE is obtained by extraction in a low ionic strength medium and subsequent complementation of the solution by salts. We wished to address whether a possible irreversible structural modification of PDE could be induced by such salt variations or by detachment of PDE from the membranes. We therefore compared two samples prepared from the same ROS suspension containing the same amounts of PDE (endogenous or purified), of membranes, and of T* (Figure 2). The first sample consisted of native ROS (circles). It was a portion of the initial ROS suspension, kept in isotonic

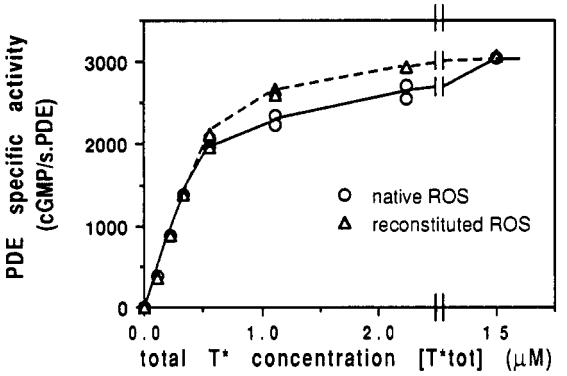

FIGURE 2: Activation by purified T* of endogenous or purified PDE. Native ROS (O) or washed membranes supplemented with PDE (Δ) were assayed for PDE activation by increasing amounts of purified T* (concentrations are indicated on the abscissa). For membrane and PDE_{tot} concentrations, see text. The ordinate gives the specific activity data. Lines: hand-fitting of the experimental data.

buffer. The second sample was reconstituted ROS (triangles). It was prepared from washed ROS and from a crude PDE extract, both components being obtained from a second portion of the initial ROS suspension. For reconstitution, the concentrated crude PDE extract was complemented with salts so as to restore the salt composition of the isotonic buffer. Then, an aliquot of washed membranes was complemented with an aliquot of the crude PDE extract so as to reach a concentration of membranes of 50 μM Rh and a maximal PDE activity equal to that of the control sample (with addition of 15 μM T*). The PDE contents of the two samples (native ROS and reconstituted ROS) were then compared, using the extraction procedure described in Experimental Procedures. We always found identical amounts of PDE in the control and reconstituted samples (0.27 μM in the present conditions). Therefore, as far as maximal activation induced by T* addition is concerned, no difference between endogenous PDE and extracted/purified PDE was present. However, a difference in behavior of endogenous and extracted/purified PDE appears when the activation of native ROS is compared to that of reconstituted ROS following addition of intermediate amounts of T* (Figure 2). In fact, the two corresponding curves overlap for low concentrations of T* (below 0.5 μM), separate for intermediate concentrations of T* (0.5–2 μM), and are again superimposed for high concentrations of T* (15 μM). Typically, at a concentration of T* of 1 μM, the PDE activity in reconstituted ROS was about 15% above that obtained with native ROS in three independent experiments. Additional experiments (not shown here) allowed us to think that the observed differences between native and reconstituted ROS are not due to the loss of another membrane component through the low-salt washing procedure, but most probably arise from a modification of PDE itself during the extraction and reconstitution procedure.

In the present study, complementation of a ROS suspension by PDE has been used only when low concentrations of T* were added.

(B) Effective Amounts of PDE Bound to ROS Membranes. PDE is a peripheral membrane-bound protein and can interact with membranes through a nonspecific attachment to the lipids (Tyminski & O'Brien, 1984), probably as a result of post-translational modifications (Catty & Deterre, 1991; Anant et al., 1992). Upon dilution of ROS membranes in isotonic buffer, PDE partitions between the bulk solution and the membranes (Liebman & Sitaramayya, 1984; Catty & Deterre, 1991).

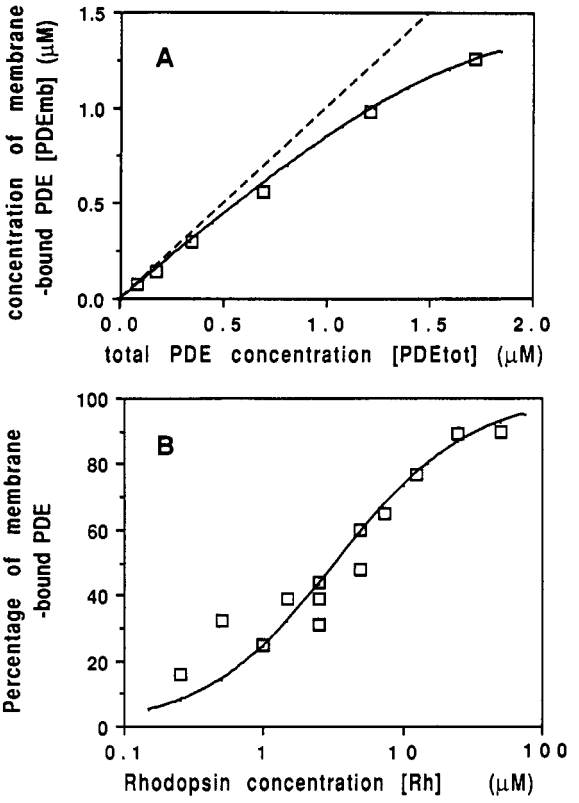

FIGURE 3: PDE binding to ROS membranes. The amounts of bound and unbound PDE in the supernatants and pellets of a centrifugation assay were determined (see Experimental Procedures). (A) Concentration of membrane-bound PDE ($[PDE_{mb}]$) as a function of the total PDE concentration ($[PDE_{tot}]$). Washed ROS membranes (62 μM Rh) were supplemented with increasing amounts of PDE (final PDE_{tot} concentrations are indicated on the abscissa). The ordinate displays the $[PDE_{mb}]$:$[PDE_{tot}]$ ratio. Solid line: fit of the data by eq 1 (Mathematical Models), with K_{PDE} = 0.14 μM and $[B_{tot}]$ = 1.6 μM. Dashed line: initial slope of the fit (which corresponds to a 1:1 ratio between $[PDE_{mb}]$ and $[PDE_{tot}]$). As the suspension did not contain T*, $[PDE_{mb}]$ is here equal to $[PDE_{mb}^0]$ defined in Mathematical Models and used in eq 5. (B) Percentage of PDE bound to ROS membranes as a function of the concentration of membranes. Two types of suspensions were used, giving similar results: native ROS suspensions (containing their endogenous pool of PDE) and washed membranes complemented with PDE at the same stoichiometry as in native ROS. The suspension was diluted with isotonic buffer so as to reach the membrane concentrations indicated on the abscissa. Solid line: fit of the data by eq 1, with K_{PDE} = 0.12 μM and $[B_{tot}]/[Rh] = 3 \times 10^{-2}$.

Two experiments were used here to determine the apparent binding constant of PDE to membranes (K_{PDE}) as well as the total amount of binding sites on the ROS membranes ($[B_{tot}]$). First (Figure 3A), increasing amounts of PDE (crude extract) were added to washed ROS membranes kept at a constant concentration (62 μM Rh). The mixture was incubated for 15 min at room temperature to allow for the equilibration of the soluble and membrane-bound pools of PDE. Soluble and membrane-bound PDE were then determined (see Experimental Procedures). The amount of bound PDE first increased linearly with added PDE and then bent toward saturation. The data, fitted with eq 1, gave $K_{PDE} = 0.14 \pm 0.02$ μM and $[B_{tot}] = 1.6 \pm 0.2$ μM; the number of PDE binding sites per rhodopsin on ROS membranes is thus $[B_{tot}] = ((2.6 \pm 0.3) \times 10^{-2})[Rh]$, which is in the same range as the value given by Tyminski and O'Brien (1984). Second (Figure 3B), suspensions of either native or reconstituted ROS were diluted in isotonic buffer to various membrane concentrations, and the amounts of soluble and membrane-bound PDE were determined. In these experiments, the ratio between PDE

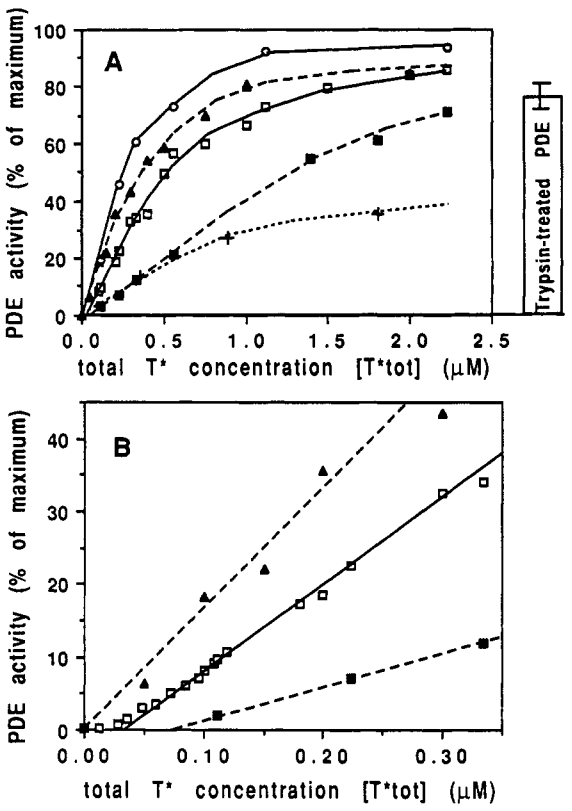

FIGURE 4: Activation by T* of endogenous PDE, as a function of the concentration of membranes. Native ROS membranes were diluted with isotonic buffer to produce a final concentration of 150 (■), 50 (□), 15 (○), 5 (▲) or 0.25 μM Rh (+). PDE was activated by addition of T* (the concentration of T^*_{tot} is indicated on the abscissa). The maximum activity was measured at 15 μM T^*_{tot}, except for the data at 0.25 μM Rh where it was deduced from the maximum activity measured on a sample prepared at 5 μM Rh. The ordinate gives the normalized PDE activity ($A_n = A/a_2[PDE_{tot}]$; see Mathematical Models). (A) Data obtained for $[T^*_{tot}]$ in the range 0–2.5 μM. Lines: hand-fitting of the experimental data. The activity of trypsin-treated PDE in an aliquot of the ROS suspension at 50 μM Rh is shown as a block to the right of panel A. (B) Data obtained for $[T^*_{tot}]$ in the range 0–0.35 μM. Lines: linear regression on the linear part of the experimental data (i.e., for $[T^*_{tot}] > 0.08$ μM for the experiment at 2 mg/mL Rh and for all values of $[T^*_{tot}]$ for the two other experiments). The intercept with the abscissa yields $[T^*_{trapped}]$ (defined in Mathematical Models).

and Rh (hence the ratio between PDE and the binding sites on the membranes) was therefore kept constant, at its physiological value of about 0.01. Fits of the data with eq 1 gave $K_{PDE} = 0.12 \pm 0.02$ μM and $[B_{tot}] = ((3 \pm 0.3) \times 10^{-2})[Rh]$. These two independent estimations of $[B_{tot}]$ yield very close values. Their mean was used in the computations.

These data show that, as soon as the membrane concentration is below 25 μM Rh (i.e., below 1 mg/mL Rh), or as soon as the total PDE concentration is not much below the binding capacity of the membranes (typically if $[PDE_{tot}] > 0.5[B_{tot}]$), the amount of PDE which is bound to the membranes, and therefore activatable by T*, cannot be taken simply as the total amount of PDE in the suspension. In the interpretation of the activation data given below, this has been systematically taken into account.

(C) Qualitative Description of the Activation of PDE by Transducin in ROS Suspensions at Various Membrane Concentrations. Figure 4A shows the activation of PDE (percentage of maximum, named A_n in mathematical models) as a function of the concentration of added T* ($[T^*_{tot}]$) in aliquots of the same initial native ROS suspension complemented with the isotonic buffer needed to reach final concentrations of 0.25 (crosses), 5 (closed triangles), 15 (open circles), 50 (open squares), and 150 μM Rh (closed squares). The activities are given as the percentage of maximal activity induced by 15 μM T^*_{tot} (except for the data at 0.25 μM Rh): this maximal specific activity of PDE was independent of the membrane concentration of the suspension and equal to 2800–3000 cGMP/(s PDE) in the present set of experiments. This complete set of experiments is representative of the results obtained from 3–5 independent determinations. The solid lines (obtained by hand fitting on the experimental data) show three important overall characteristics of these activation curves.

The first characteristic deals with the shapes of the curves (Figure 4A). In the intermediate range of membrane concentration (5–50 μM Rh) one can clearly observe a linear part in these curves (from 0 to about 60% of maximal activity as T* increases from 0 to 0.5 μM), which then bends toward a slowly raising phase, finally reaching maximal activity (see also Figures 1 and 2). In this range of membrane concentration, the normalized response of PDE to T* is only slightly modified by changes in ROS concentration. On the contrary, for both the highest (150 μM Rh) and the lowest (0.25 μM Rh) ROS concentrations tested, the normalized activity at 0.5 μM T^*_{tot} is much lower than for the intermediate range of ROS concentrations. However, the reasons for this behavior are likely to be specific to each case. At high ROS concentrations, on the one hand, the concentration of PDE is higher than 0.5 μM (typically 1 μM at a ROS concentration of 150 μM Rh), and concentrations of T^*_{tot} higher than 0.5 μM are therefore needed to titrate PDE. At low ROS concentrations, on the other hand, a nonnegligible pool of PDE is soluble in the absence of T* (typically 80% at a ROS concentration of 0.25 μM Rh; see Figure 3B). The activation of PDE is thus much less efficient.

The second characteristic deals with the shapes of the curves at very low additions of T* (Figure 4B). The linear increase of PDE activity described above does not actually start immediately from $[T^*_{tot}] = 0$. The extrapolation of the linear part of the activation curve intercepts the abscissa at a concentration of T^*_{tot} which decreases with decreasing concentration of membranes in the experiment (typically, 75 nM at 150 μM Rh, 25 nM at 50 μM Rh, and not detectable at or below 5 μM Rh). A small amount of T* appears to be ineffective in activating PDE. It is probably due to high-affinity binding of T* to a component of ROS membranes present in limited amounts (1/2000 relative to Rh). No attempt was made to further characterize this small binding capacity. We corrected T^*_{tot}, especially when low concentrations of T^*_{tot} and high concentrations of membranes were under consideration, by subtracting the corresponding amount of $T^*_{trapped}$ from this value.

The third characteristic of the activation curves deals with the maximal activity, obtained at 10–15 μM T* for the intermediate membrane concentration range (Figure 4A, open circles and squares, closed triangles). It was always about 20% higher than the activity obtained by trypsin treatment of PDE (see block in Figure 4A). In all curve fittings, this maximal activity was therefore taken as 100%, in contrast to most of the previous work, where the activity of a trypsin-treated sample was used for normalization.

(D) Determination of the Activation Parameters of PDE by T from Experiments on ROS Suspensions in the Concentration Range 5–150 μM Rh.* For membrane concentrations ranging from 5 to 150 μM Rh, the amount of PDE which partitions to the solution (in the absence of T*) is never

Table 1: Scores of Some Fits of Experiments Carried Out at Membrane Concentrations from 5 to 150 μM Rh[a]

	parameter			concentration (μM Rh)			
model[b]	α	K_1 (μM)	K_2 (μM)	5	15	50	150
A							
	1	0.15		19	27	68	244
	1	0.3		130	241	7	88
	1	0.7		678	978	209	3
B							
	0.3	0.075	0.22	45	57	63	50
	0.3	0.1	0.6	75	411	196	100
C							
	0.9	0.4	0.15	38	40	40	39

[a] Experimental data of Figure 4. Theoretical activities were calculated at four membrane concentrations using eqs 2–4 (Mathematical Models). The mean values of K_{PDE} (0.13 μM) and $B_{tot}/[Rh]$ (2.8×10^{-2}) are determined from Figure 3. The experimental total PDE concentrations were deduced from the experimental equation $[PDE_{tot}/[Rh] = 0.8 \times 10^{-2}$ (see Figure 3). Scores (see Mathematical Models) of the fit of the experimental data for chosen sets of binding and activity parameters (K_1, K_2, α) are given in the rightmost four columns. [b] A: Model in which one T* binds to PDE and fully activates it (α = 1). For the calculations, K_2 was set to 100 μM. B and C: Models in which two T*'s bind to PDE, the first eliciting a partial PDE activation α. B: Parameters as in Bennett and Clerc (1989) and Clerc and Bennett (1992). C: Parameters deduced from our experiments and used in the theoretical activation curves shown in Figure 6.

above 50% (see Figure 3B). Moreover, addition of T* leads to an increase in membrane binding of PDE (Catty et al., 1992). We are therefore (as we have confirmed) working in conditions under which little or no PDE activity is present in the soluble fraction of the suspension. The model used for the mathematical calculations (eqs 2–4 in Mathematical Models) introduces the true value of $[PDE_{mb}]$ (derived from $[PDE_{tot}]$ via the binding curves given in Figure 3) and takes into account that addition of T* induces more binding of PDE to the membrane via the formation of the PDE_{mb}–T* complexes. This model should then be applicable to the whole range of membrane concentrations. We present here the analysis of the complete set of experiments presented in Figure 4A. The error range given below for the parameters K_1, K_2, and α will take into account the uncertainty arising from the mathematical fit of this particular experiment and the uncertainty arising from the variability between different sets of experiments.

The validity of our model is assessed with respect to the possibility of finding a set of parameters α, K_1, and K_2 that allow a good fit to the experimental data (PDE activation curves) obtained at four membrane concentrations: 5, 15, 50, and 150 μM Rh (Figures 1 and 4A). For each tested set of parameters, we calculated the E^2 scores corresponding to the fits, and rejected the sets of parameters for which E^2 was above 50 (see Mathematical Models).

We first tested whether the data could be fitted by a model in which only one T* would bind to PDE and activate it. As shown in Table 1, different values of K_1 allowed one to individually fit the different curves obtained at different membrane concentrations, but no single value of K_1 could simultaneously fit all data. This confirms that the binding of two T* to PDE is necessary to explain the activation of PDE by T*.

We then screened for acceptable sets of parameters: at different representative values of α (from 0.1 to 0.9), we determined domains in the (K_1, K_2) space in which the set of parameters α, K_1, and K_2 was acceptable. In Figure 5A, these domains correspond to the interior of the drawn boundaries.

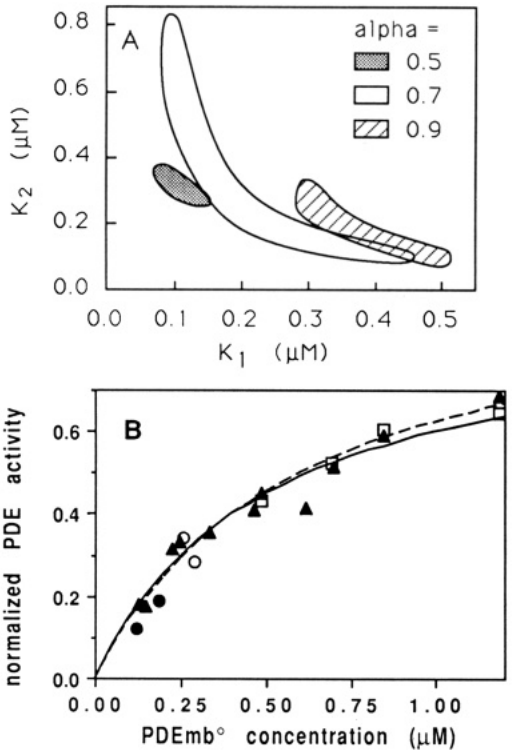

FIGURE 5: Determination of the α, K_1 and K_2 parameters of PDE activation by T*. (A) Determination of domains for α, K_1, and K_2 from activation of PDE over a range of T^*_{tot} concentrations. Experimental data for membrane concentrations of 5, 15, 50, and 150 μM Rh (taken from Figure 4A) were fitted using eqs 2–4 (Mathematical Models), the parameters describing PDE binding to the membranes determined in Figure 3 (K_{PDE} = 0.13 μM and $[B_{tot}]/[Rh] = 2.8 \times 10^{-2}$), and the experimentally determined total PDE concentrations ($[PDE_{tot}]/[Rh] = 0.8 \times 10^{-2}$). For each selected value of α, the acceptable values for K_1 and K_2 (giving scores $E^2 < 50$ for each condition of membrane concentration) lay inside the drawn boundaries. (B) Determination of α and K_1 through activation of PDE by submicromolar amounts of T*. Four types of suspensions were used: native ROS (○), PDE-depleted ROS (●), native ROS supplemented with purified PDE (□), and washed membranes supplemented with purified PDE (▲). All assays were performed at a final membrane concentration of 50 μM Rh and with the addition of 0.12 μM T^*_{tot}. The data shown are the results of four independent experiments. The activity data (amount of cGMP hydrolyzed/s) were normalized to a specific maximal activity of 3000 cGMP/(s PDE) and divided by the concentration of activator (see text); the corresponding number, given on the ordinate, has no dimension. The abscissa gives the concentration of membrane-bound PDE in the absence of T* ($[PDE_{mb}^0]$ (see Mathematical Models) determined from the total amount of PDE in the suspension ($[PDE_{tot}]$) using the results from Figure 3B. Lines: fitting of the data to eq 5 with α = 0.9 and K_1 = 0.5 (solid line) or α = 1 and K_1 = 0.6 (dashed line).

As soon as α was higher than 0.5, a large number of possibilities could be found for the values of K_1 and K_2. For α = 0.3 however, the values of K_1 and K_2 reported by Clerc et al. (1992), but not those reported by Bennett and Clerc (1989), resulted in a fit that was close to acceptable (see Table 1).

To discriminate between all these acceptable fits, we searched for more precise information on the parameters for the first binding of T* to PDE, i.e., K_1 and α. We therefore used data from experiments in which low amounts of T^*_{tot} were added to ROS containing variable amounts of PDE (Figure 5B). In these conditions where the concentration of PDE is much higher than that of T^*_{free}, the T*–PDE_{mb} complexes (containing only one bound T*) are essentially the only complexes formed and the contribution of the T*–PDE_{mb}–T* complexes is negligible. Thus, the normalized PDE activity (named A_n' in Mathematical Models) is simply related to the concentration of membrane bound PDE in the absence of

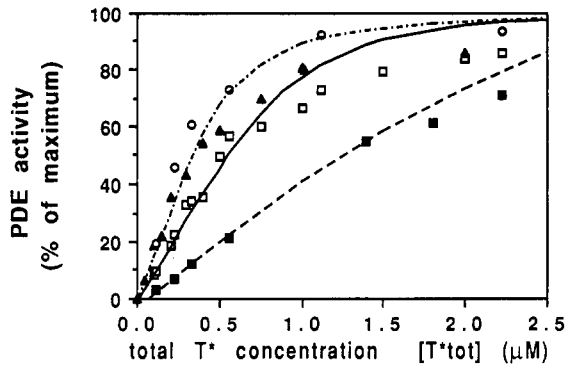

FIGURE 6: Fits of PDE activation by T* at membrane concentrations of 5, 15, 50, and 150 μM Rh for the selected set of parameters α = 0.9, K_1 = 0.4 μM, and K_2 = 0.15 μM. The data for PDE activation by T* at membrane concentrations of 150 (■), 50 (□), 15 (○), and 5 μM Rh (▲) are taken from Figure 4A. Fits were performed using eqs 2–4 (see Mathematical Models) and the following parameters: K_{PDE} = 0.13 μM, $[B_{tot}]/[Rh] = 2.8 \times 10^{-2}$, $[PDE_{tot}]/[Rh] = 0.8 \times 10^{-2}$, α = 0.9, K_1 = 0.4 μM, and K_2 = 0.15 μM. Dashed line: [Rh] = 150 μM. Solid line: [Rh] = 50 μM. Dot-dashed line: [Rh] = 15 μM Rh. The theoretical curve at 5 μM Rh, which was almost superimposable with that at 15 μM Rh, was omitted for clarity.

T^*_{tot} ($[PDE_{mb}^0]$; see eq 5). The concentration of PDE in native ROS suspensions can in principle be manipulated in two ways: (i) addition of purified PDE (this is valid because the activation curve is studied at low T*; see Figure 2); (ii) depletion of PDE by washes in isotonic buffer at low membrane concentration, a procedure in which PDE is allowed to be partially detached from the membranes (see Figure 3B). The experiments given in Figure 5B concern four types of samples, all of them brought to a final membrane concentration of 50 μM Rh: native ROS (with their native PDE content, open circles), ROS depleted of PDE (closed circles), native ROS supplemented with purified PDE (open squares), and washed membranes supplemented with purified PDE (closed triangles). The total amount of PDE in each sample was determined as explained in Experimental Procedures. The PDE activity of all these samples was elicited by addition of 0.12 μM T^*_{tot}. The given activities (A) are normalized (A_n'; see Mathematical Models) to a specific maximal activity of 3000 cGMP/(s PDE) (see Figure 2) and divided by the concentration of activator (equal to $[T^*_{tot}] - [T^*_{trapped}]$; $[T^*_{trapped}]$ is 25 nM in this case; see Figure 4B). The ordinate in Figure 5 therefore represents the normalized slope of the linear initial part of the activation curve of PDE by T*. The results are plotted as a function of $[PDE_{mb}^0]$ (concentration of membrane-bound PDE at $[T^*_{tot}] = 0$; see eq 5), which is deduced from $[PDE_{tot}]$ using the binding characteristics of PDE illustrated in Figure 3. The curve in Figure 5 is described by a hyperbola (see eq 5) with an asymptote at α for $[PDE_{mb}^0] \rightarrow \infty$. Experimental points clearly exist for PDE activities above 0.5 (in the given units), and therefore α is necessarily above 0.5. The mathematical fit by eq 7 resulted in $K_1 = 0.5 \pm 0.1$ μM and $0.8 < \alpha < 1$. This is clearly contradictory to the data of $\alpha = 0.3$ given by Clerc et al. (1992). Indeed, these authors failed to subtract the amount of $[T^*_{trapped}]$ (25 nM or more in their case) from $[T^*_{tot}]$ (80 nM in their case). They therefore underestimated the PDE activity in the normalized units used in this description by a factor of at least 1.5.

Taking together the constraints for α, K_1, and K_2 obtained from Figure 5, the best acceptable set of parameters appears to be α = 0.8–0.9, K_1 = 0.4–0.5 μM, and K_2 = 0.1–0.2 μM. The corresponding scores are given in Table 1, and the fits are displayed, together with the experimental data, in Figure 6. We then checked that the data of Figure 5B could be fitted, without any approximation, with this set of K_1, K_2, and α values (not shown).

The above modeling is visibly better for the initial slope of the activation curve than for T^*_{tot} concentrations in the range 1–3 μM. In this range, the calculated activities were always higher than experimentally observed. The hypothesis of T* functioning as an oligomer (Wessling-Resnick & Johnson, 1987) cannot correct this discrepancy, as the calculated PDE activity at high $[T^*_{tot}]$ would then be higher than in our model. Moreover, several reports (Fung et al., 1981; Hingorani et al., 1988) show evidence that T* is monomeric in conditions similar to those of our study.

DISCUSSION

In vertebrate rods, the α-subunit of transducin loaded with GTP (T*) interacts with a cGMP phosphodiesterase (PDE) to activate it (Chabre & Deterre, 1989). Several lines of evidence support the assumption that the activation of PDE implies the successive binding of two T* [reviewed in Pfister et al. (1993)], and indeed, the activation of PDE by T* cannot be fitted with only one equilibrium (Table 1). In our model, a first T* binds to PDE, with an apparent binding constant K_1, and elicits in the T*–PDE_{mb} thus formed a normalized PDE activity denoted α; a second T* then binds to T*–PDE_{mb}, with a constant K_2, and the complex formed, T*–PDE_{mb}–T*, then reaches its maximal PDE activity, i.e., 1 in normalized units. The aim of the present work was to describe the characteristics of these two successive bindings, taking properly and completely into account the influence of the membranes on this process.

*Activation of PDE by the Successive Binding of 2 T*s on the Surface of ROS Membranes.* It has been shown that the presence of membranes greatly enhanced the activation of PDE by T* (Fung & Nash, 1983; Liebman & Sitaramayya, 1984; Tyminski & O'Brien, 1984; Phillips et al., 1989; Bennett & Clerc, 1989). PDE itself interacts peripherally with the membrane (or with lipids) via nonspecific sites (Tyminski & O'Brien, 1984; Liebman & Sitaramayya, 1984; Catty et al., 1991; our Figure 3), and both the PDE:Rh ratio and the absolute membrane concentration determine the relative abundance of these two pools. Therefore, the effect of membranes on the extent of PDE activation by T* can be described here essentially as related to the relative abundance of the membrane-bound pool of PDE. We specifically took into account our observation that the activation of PDE by T* occurred only on the membranes and not in the bulk solution (except possibly at a low membrane concentration, ≤1 μM Rh).

To check our model concerning the influence of membranes on the activation of PDE by T*, we carried out experiments over a wide range of membrane concentrations (from 0.25 to 150 μM Rh; see Figure 4). In these experiments, the ratio PDE:Rh was kept constant, using the value characteristic of the native ROS (about 0.01). The overall shapes of the activation curves $A_n = f([T^*_{tot}])$ display two phases, most clearly visible in the intermediate range of membrane concentrations (Figure 4A): a linear initial increase is followed by a slow rise which continues to concentrations of T^*_{tot} as high as 10–15 μM. The activity thus reached was about 120% of the activity of an aliquot activated by trypsin treatment. Therefore, in the present work, activities were normalized to the value obtained by addition of 15 μM T*. We could reject the hypothesis that the biphasic shape observed in the curves in Figure 4 would be due to the existence of two pools of purified T*, one being more effective at activating PDE

(Malinski & Wensel, 1992), since we observed that the endogenous pool of T, activated by GTPγS, was as effective as purified T* at the same concentration (Figure 1). However, for very low T* concentrations, it appeared that a portion of T^*_{tot} remained ineffective, probably by being trapped in the membranes (Figure 4B). This amount did not exceed 25 nM at a membrane concentration of 50 μM Rh. This value is negligible for the data displayed in Figure 4A, but had to be taken into account in experiments performed at low concentrations of T^*_{tot} (Figure 5B).

The activation curves in Figure 4 (in the membrane concentration range 5–150 μM Rh) as well as the data in Figure 5B were modeled assuming that only the membrane-bound pool of PDE is activatable, that T* is monomeric, and that the T*–PDE_{mb} and T*–PDE_{mb}–T* complexes formed are totally membrane-bound. This was supported by the observation that no detectable PDE activity was present in the soluble fraction. We found that all the data were consistent, within about 10%, with the following set of constants: K_1 = 0.4–0.5 μM, K_2 = 0.1–0.2 μM, and α = 0.8–0.9.

The first major finding of this study is that in the complex T*–PDE_{mb} (i.e., the intermediate complex containing only one T* bound) the activity of PDE would be nearly maximal. This is contradictory to the findings of Clerc et al. (1992) who described this complex as having only 30% of the maximal PDE activity. This discrepancy originates mainly from the data used to obtain K_1 and α [Figure 5B in the present work; Figure 1 in Clerc et al. (1992)]. Clerc et al. observed that the PDE activity (induced by 80 nM T^*_{tot}) sharply saturates, for PDE_{tot} > 0.2 μM, and reaches about 30% of maximum. By contrast, we observed that the PDE activity (induced by 100 nM T^*_{tot}) increased steadily with additions of PDE up to micromolar amounts. The highest PDE activity experimentally reached was as high as 60% of maximum, which still did not correspond to saturation. Several explanations can be put forward. First, at the low concentrations of T^*_{tot} used in these experiments, some T* is trapped and is therefore unable to activate PDE. Neglecting the corresponding correction leads to an underestimate of α by about 45%. Second, Clerc et al. analyzed their data as a function of the total amount of PDE added (PDE_{tot}), whereas only membrane-bound PDE (PDE_{mb}) is efficiently activatable. Even at a membrane concentration of 50 μM Rh, and even if PDE_{tot} stays below the total amount of binding sites on the membrane (B_{tot}), one cannot consider that all PDE added becomes membrane-bound (see Figure 3). Furthermore, the total number of binding sites on the membrane (B_{tot}) limits the experimentally available concentration of PDE_{mb}, whatever the total concentration of PDE. Failure to take into account the equilibrium PDE_{sol} + empty sites ↔ PDE_{mb} (see Mathematical Models) will lead to an underestimate of α as well as of K_1. However, an estimation of the exact corrections to be introduced in the data of Clerc et al. would require an exact knowledge of the binding characteristics of PDE to the membranes in their experimental conditions.

The second major finding of our study is that the binding of T* to PDE is cooperative: the binding of the second T* to T*–PDE_{mb} appears to have a higher apparent affinity constant (0.1–0.2 μM) than the binding of the first T* to PDE_{mb} (0.4–0.5 μM). This again is not in accordance with Clerc et al. (1992). In more indirect experiments, apparent binding constants of much lower values have been suggested. Erickson and Cerione (1991) determined a value of 21 nM from resonance energy transfer between labeled T* and PDE, and Heck and Hofmann (1993) reported a value of less than 2.5 nM, as determined from light scattering changes of ROS suspensions. However, the conditions for the assays used in both of these studies favor the existence of interactions between T* and PDE in the soluble phase [no membranes in Erickson and Cerione (1991); very low membrane concentration and relatively high PDE concentration in Heck and Hofmann (1993)]. The interaction would thus essentially concern T* and PDEγ, for which the binding constant, as determined by intrinsic fluorescence changes of T*, is lower than 0.1 nM (Otto-Bruc et al., 1993). A comparison with the results given in Malinsky and Wensel (1992) has no relevance here, as these authors suppose that (i) only part of T* is potent to activate PDE and (ii) only one T* binds to PDE.

PDE Activation by T in Situ.* In intact bovine rods, the tightly packed flat discs leave little cytoplasmic volume, and the equivalent membrane concentration is about 5 mM. The corresponding concentrations of T and PDE are about 500 and 50 μM, respectively, and the PDE pool is entirely membrane-bound. Our mathematical model (eqs 2–4) is therefore appropriate to describe PDE activation by T*, provided extrapolation of the structural and kinetic properties of T* and PDE remains valid at those concentrations, which are much higher than those used in the present study.

In response to one photon, 500 T*s are created in 1 s (Bruckert et al., 1992) in the interdiscal space near the Rh* that forms. The corresponding concentration of T* can reach 80 μM, i.e., the same order of magnitude as the number of T* sites on PDE (about 100 μM). T*–PDE_{mb} and T*–PDE_{mb}–T* complexes will then be formed, but due to the cooperative binding of T* on PDE, T*–PDE–T* will be the main species (about 90% of total PDE_{mb} and T* complexes). From an estimate of the specific activity of T*–PDE as 2500–2700 cGMP/(s T*–PDE) (maximal activity, 2800–3000 cGMP/(s PDE); α = 0.9; see Results), the corresponding hydrolysis rate of cGMP would be on the order of 150 mM/s. It is noteworthy that, under faint illumination, the amplitude of the PDE activity elicited would depend linearly on the amount of T* formed up to 100 μM. Following a very bright flash, several rhodopsins are photoexcited in one disc, and the concentration of activated transducin can reach a few hundred micromolar. Nonetheless, according to our results, this will not induce a much higher PDE activity. Possibly this maximal activity could be reached faster because of the higher concentrations of T*; however, the kinetic parameters for the association and dissociation of these complexes remain to be determined.

The physiologically activated PDE thus appears to be in a complex with two T*s. Bennett and Clerc (1989) suggested that the low catalytic activity of the T*–PDE complex and a noncooperative binding put a threshold on PDE activation, protecting it from spontaneous, light-independent (albeit improbable) transducin activation. Our results do not confirm this interesting hypothesis. The physiological role of the binding of two T*s to PDE could mainly reside in the deactivation of T* itself: Pagès et al. (1992, 1993) showed that T* hydrolyzes its bound GTP at a rate that is 4–10 times faster when T* can interact with PDE than when it is free in solution; Angleson and Wensel (1993) show that this would be due to the presence, in the disc membrane, of a GTPase activating factor. Whatever the exact mechanism, the presence of two sites for binding of T* on PDE would potentially double the probability of a fast deactivation of T*.

ACKNOWLEDGMENT

The authors thank C. Roche and F. Picaretta for expert technical assistance, J. C. Pfister for help in running the

Mathematica software, N. Bennett for fruitful discussion, and R. Margolis for correcting the manuscript.

REFERENCES

Anant, J. S., Ong, O. C., Xie, H., Clarke, S., O'Brien, P. J., & Fung, B. K.-K. (1992) *J. Biol. Chem. 267,* 687–690.

Angleson, J. K., & Wensel, T. G. (1993) *Neuron 11,* 939–949.

Bennett, N., & Clerc, A. (1989) *Biochemistry 28,* 7418–7424.

Bruckert, F., Chabre, M., & Vuong, T. M. (1992) *Biophys. J. 63,* 616–629.

Catty, P., & Deterre, P. (1991) *Eur. J. Biochem. 199,* 263–269.

Catty, P., Pfister, C., Bruckert, F., & Deterre, P. (1992) *J. Biol. Chem. 267,* 19489–19493.

Chabre, M., & Deterre, P. (1989) *Eur. J. Biochem. 179,* 255–269.

Clerc, A., & Bennett, N. (1992) *J. Biol. Chem. 267,* 6620–6627.

Clerc, A., Catty, P., & Bennett, N. (1992) *J. Biol. Chem. 267,* 19948–19953.

Compton, S. J., & Jones, C. G. (1985) *Anal. Biochem. 151,* 369–374.

Deterre, P., Bigay, J., Pfister, C., & Chabre, M. (1984) *FEBS Lett. 178,* 228–232.

Deterre, P., Bigay, J., Robert, M., Pfister, C., Kühn, H., & Chabre, M. (1986) *Proteins: Struct., Funct., Genet. 1,* 188–193.

Deterre, P., Bigay, J., Forquet, F., Robert, M., & Chabre, M. (1988) *Proc. Natl. Acad. Sci. U.S.A. 85,* 2424–2428.

Erickson, J. W., & Cerione, R. A. (1991) *Biochemistry 30,* 7112–7118.

Fung, B. K.-K., & Nash, C. R. (1983) *J. Biol. Chem. 258,* 10503–10510.

Fung, B. K.-K., Hurley, J. B., & Stryer, L. (1981) *Proc. Natl. Acad. Sci. U.S.A. 78,* 152–156.

Fung, B. K.-K., Young, J. H., Yamane, H. K., & Griswold-Prenner, I. (1990) *Biochemistry 29,* 2657–2664.

Heck, M., & Hofmann, K. P. (1993) *Biochemistry 32,* 8220–8227.

Hingorani V. N., Tobias D. T., Henderson J. T., & Ho Y. K. (1988) *J. Biol. Chem. 263,* 6916–6926.

Kühn, H. (1981) in *Current Topics in Membrane and Transport* (Miller, W. H., Ed.) Vol. 15, pp 171–201, Academic Press, New York.

Liebman, P. A., & Evanczuk, A. T. (1981) *Methods Enzymol. 81,* 532–542.

Liebman, P. A., & Sitaramayya, A. (1984) in *Advances in Cyclic Nucleotides and Phosphoprotein Research 17* (Greengard, P., et al., Eds.) pp 215–225, Raven Press, New York.

Lipkin, V. M., Khramtsov, N. V., Vasilevskaya, I. A., Atabekova, N. V., Muradov, K. G., Gubanov, V. V., Li, T., Johnston, J. P., Volpp, K. J., & Applebury, M. L. (1990) *J. Biol. Chem. 265,* 12955–12959.

Malinski, J. A., & Wensel, T. G. (1992) *Biochemistry 31,* 9502–9512.

Otto-Bruc, A., Antonny, B., Vuong, T. M., Chardin, P., & Chabre, M. (1993) *Biochemistry 32,* 8636–8645.

Pagès, F., Deterre, P., & Pfister, C. (1992) *J. Biol. Chem. 267,* 22018–22021.

Pagès, F., Deterre, P., & Pfister, C. (1993) *J. Biol. Chem. 268,* 26358–26364.

Pfister, C., Bennett, N., Bruckert, F., Catty, P., Clerc, A., Pagès, F., & Deterre, P. (1993) *Cell. Signalling 5,* 235–251.

Phillips, W. J., Trukawinski, S., & Cerione, R. A. (1989) *J. Biol. Chem. 264,* 16679–16688.

Stryer, L. (1991) *J. Biol. Chem. 266,* 10711–10714.

Tyminski, P. N., & O'Brien, D. F. (1984) *Biochemistry 23,* 3986–3993.

Wensel, T. G., & Stryer, L. (1986) *Proteins: Struct., Funct., Genet. 1,* 90–99.

Wensel, T. G., & Stryer, L. (1990) *Biochemistry 29,* 2155–2161.

Wessling-Resnick, M., & Johnson, G. L. (1987) *J. Biol. Chem. 262,* 3697–3705.